



Cite this: *Chem. Commun.*, 2024, **60**, 1265

Received 30th October 2023,
Accepted 28th December 2023

DOI: 10.1039/d3cc05331h

rsc.li/chemcomm

In this manuscript, a photoinduced ligand-to-metal charge transfer (LMCT) approach, employing transition-metal-based photocatalysts, for the efficient alkylation of electron-poor olefin is described. The developed redox-neutral process benefits from mild reaction conditions and involves a wide range of chromone-3-carboxylic acids as well as nucleophiles amenable to selective C–H functionalization leading to the formation of 2-substituted chroman-4-one compounds with potential biological activity.

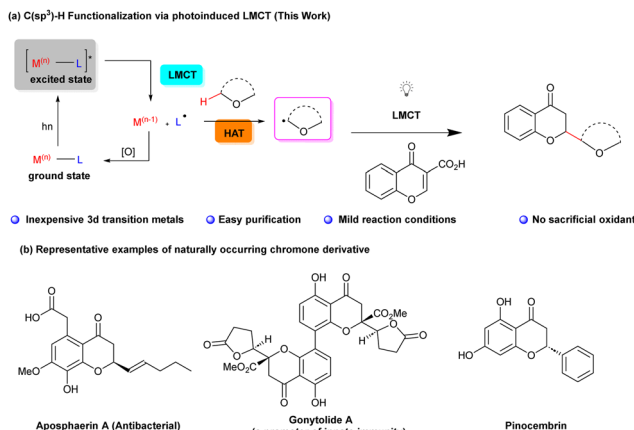
The selective functionalization of aliphatic carbon–hydrogen (C–H) bonds has been a longstanding pursuit in the realm of organic synthesis.^{1,2} While the functionalization of sp^2 and activated sp^3 C–H bonds using transition metal catalysts is a well-established field,³ addressing the challenges associated with inert sp^3 –H functionalization has been proven to be a complex endeavour, marked by issues related to selectivity.⁴ Recently, considerable efforts in this domain, driven by the application of 4d or 5d transition metal catalysts (mostly Pd, Ru, and Rh), have been made. Remarkably, 3d transition metals, appreciated for their environmental and economic benefits, also contributed significantly to the functionalization of otherwise inert sp^3 –H bonds.^{3a,5} Among these, copper (Cu) stands out due to its abundance and versatile redox reactivity, stemming from its array of oxidation states and its ability to coordinate with π -bonds and heteroatoms.^{3a,5,6}

An interesting strategy to sp^3 –H functionalization is the photoinduced radical-mediated hydrogen atom transfer (HAT) (Scheme 1a). This approach enables the selective introduction of functional groups into molecules by generating alkyl radicals as versatile intermediates, thereby avoiding the need for pre-functionalization or the use of directing groups.^{7,8} The efficacy

of HAT depends on the intricate interplay of electronic and steric factors of both sp^3 –H bonds within the substrate as well as of the HAT reagent itself.^{9,10} Cyclic and acyclic ethers constitute particularly interesting groups of reactants in such transformations due to their ability to undergo selective transformation with participation of the electron-rich sp^3 –H bonds adjacent to the oxygen atom.¹¹

Interestingly, photoinduced ligand-to-metal charge transfer (LMCT) has been found to promote radical-mediated processes, thus bypassing more traditional photoredox processes.¹² It was demonstrated that by direct excitation of high-valency metal–ligand complexes the formation of highly reactive radical species was possible. These key intermediates subsequently participate in the intermolecular HAT processes with hydrocarbons opening exciting possibilities in modern organic synthesis.^{13,14} In 2019 the Rovis group made a groundbreaking discovery by demonstrating that Co(II)-acetylides possessed the capability to engage in the LMCT process, effectively promoting [2+2]-cycloadditions with alkynes.¹⁵

Building upon this pivotal advancement and driven by the hypothesis that other air-stable metal salts could complement



Scheme 1 Cu-catalyzed LMCT enables unactivated sp^3 –H alkylation.

^a Institute of Organic Chemistry, Faculty of Chemistry, Łódź University of Technology, Źeromskiego 116, 90-924 Łódź, Poland

^b Institute of General and Ecological Chemistry, Faculty of Chemistry, Łódź University of Technology Źeromskiego 116, 90-924 Łódź, Poland.

E-mail: anna.albrecht@p.lodz.pl

† Electronic supplementary information (ESI) available. See DOI: <https://doi.org/10.1039/d3cc05331h>



HAT-based methodologies in enhancing substrate diversity, selectivity, and reactivity, our research endeavours took a significant leap forward. We initiated an extensive exploration into the potential of various metal halides to participate in LMCT. Our research was also inspired by the pioneering work of Kochi, who demonstrated the utility of cupric chloride in the stoichiometric chlorination of alkanes in acetonitrile.¹⁶ Furthermore, Rovis and Tarnovsky demonstrated the utility of various photoactive species capable of undergoing ligand-to-metal charge transfer (LMCT) within Cu(II) chlorocomplexes in acetonitrile.¹⁷

Inspired by these research studies, we decided to turn our attention to the potential of photoinduced LMCT using earth-abundant transition-metal-based photocatalysts. Through an exploration of photoinduced HAT and the role of chloride salts, we decided to perform a photoactivation-based site-specific tandem C(sp³)-H functionalization/decarboxylation reaction of chromone-3-carboxylic acids, leading to the formation of 2-substituted chroman-4-ones (Scheme 1a). In this context it is worth noting that chromanones and related compounds (Scheme 1b) constitute privileged structural motifs present in many natural products and exhibit a wide variety of biological activities.¹⁸ Selected examples of natural flavanones and chromanones are shown in Scheme 1 featuring notable members like aposphaerin A (recognized for its antibacterial properties)^{19a} and gonytolide A (a promoter of innate immunity).^{19b-d} Furthermore, flavonoid pinocembrin is associated with mitigating the risk of specific chronic diseases.²⁰

Decarboxylative Michael reaction based on the nucleophilic addition to carboxylic-acid-activated olefins followed by the decarboxylation reaction constitute a powerful synthetic tool.²¹

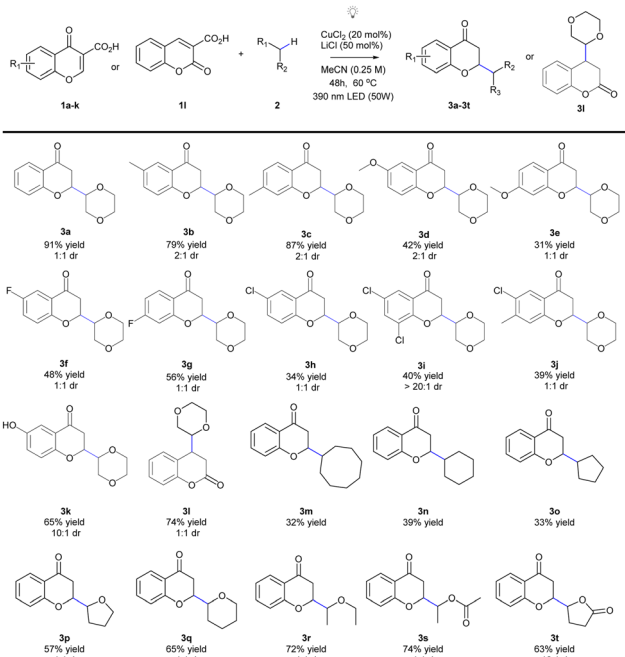
Recently, we described the photocatalytic, doubly decarboxylative Giese reaction applicable to a wide range of carboxylic acids^{22a} and visible-light driven reductive azaarylation of coumarin-3-carboxylic acids,^{22b} thus demonstrating the potential of decarboxylative radical strategies. Initially, the optimization studies were performed using chromone-3-carboxylic acid **1a** and 1,4-dioxane **2a** as model substrates and it was found that it is possible to realize the devised synthetic strategy in the presence of 20 mol% of anhydrous CuCl₂ as the catalyst and 50 mol% of LiCl in acetonitrile, under an argon atmosphere and utilizing 390 nm LEDs (as they excite synthetically useful LMCT absorption bands) at an elevated temperature of 60 °C for 48 hours. The outcome was remarkable yielding the exclusive, regioselective formation of the 2-substituted chroman-4-one **3a** with a good yield of 83%. This approach was systematically explored in order to fine-tune the critical parameters, resulting in the conditions necessary for achieving the desired outcome in this study. One notable enhancement was the utilization of a well-sealed crimp vial instead of a screw-capped vial, which led to a substantial increase in the yield, reaching to 91% (Table 1, entry 1). The utilization of 10-fold excess of **2a** resulted in a decreased yield of the desired product **3a** (Table 1, entry 2). Throughout these optimization studies, the optimal **1a**:**2a** ratio (1.0:5.0 equiv.) was the most favourable for achieving good results. It became evident that these selected parameters encompassed the ideal conditions to enable LMCT within a redox-neutral Giese-type coupling reaction.²³

Table 1 Optimization and control studies

Entry	Deviation from standard conditions	dr	Yield (%)
1	None	1:1	91
2	10.0 (equiv.) 2a	1:1	21
3	Acetone	1:1	65
4	TMSCl	1:1	60
5	RuCl ₃	1:1	79
6	FeCl ₃	1:1	70
7	CH ₃ CN (0.3 M)	1:1	57
8	0% CuCl ₂	n.d.	<5
9	In the dark	n.d.	<5
10	Kessil (440 nm)	1:1	37

All reactions were performed in a crimp vial using **1a** (0.1 mmol), **2a** (0.5 mmol), CuCl₂ (20 mol%), LiCl (50 mol%), anhydrous MeCN [0.25 M], 50 W blue LED irradiation (390 nm), and a 7 cm distance from the vial at 60 °C for 48 h. TMSCl = trimethylsilyl chloride; yields of isolated product **3a** are reported after chromatographic purification. dr – diastereoisomeric ratio

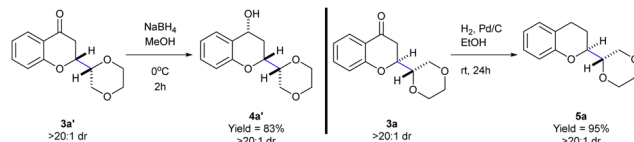
Furthermore, the influence of solvents on the reaction outcome was evaluated and identified that anhydrous acetonitrile is the pivotal solvent for enhancing the efficiency of the proposed coupling of inactivated C(sp³)-H bonds with electron-deficient olefins. Alternative solvents like acetone, DMF, CH₂Cl₂, and CHCl₃ (as indicated in Table 1, entry 3, and details in ESI,† Table S2) exhibited substantially reduced effectiveness, resulting in notably lower yields (65%, 16%, 13%, and 9%, respectively). To increase the redox-neutral transformation, an exogenous chloride source in conjunction with catalytic amounts of CuCl₂ was introduced. Application of TMSCl (as denoted in Table 1, entry 4) and TBACl (see ESI,† Table S3) in both cases demonstrated comparable efficiency, affording the desired product with 60% and 53% yields, respectively. Notably, the presence of HCl did not yield any product (see ESI,† Table S3). In the course of further studies, alternative LMCT catalysts such as RuCl₃ and FeCl₃ as photocatalysts were tested (Table 1, entries 5 and 6). These catalysts delivered product **3a** in 79% and 70% yield, respectively, and did not provide a significant improvement over CuCl₂. In contrast, TiCl₄ and BiCl₃ had a dramatically adverse impact on the reaction outcome (ESI,† Table S4). Turning our attention to solvent concentration, we found that CH₃CN (0.3 M) (Table 1, entry 7) provided the desired product in 57% yield. Control experiments pointed out the indispensability of CuCl₂ and shed light on this transformation (Table 1, entries 8 and 9). Diminished yields were observed when 440 nm irradiation was employed (Table 1, entry 10). The best results were obtained using 5-fold excess of **2a** with respect to **1a** with application of 20 mol% of CuCl₂ as a catalyst, 50 mol% of LiCl in acetonitrile and irradiation of the reaction mixture for 48 h at 60 °C (Table 1, entry 1). Under these conditions **3a** was obtained in 91% yield as a separable mixture of two diastereoisomers in a 1:1 ratio (see the ESI,† for the assignment of the relative configuration). With optimized



Scheme 2 Scope of the reaction.

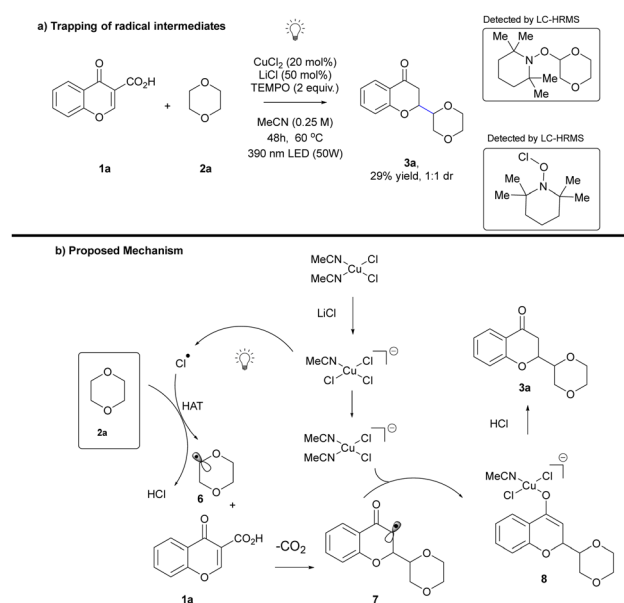
reaction conditions in hand, the scope of this photocatalytic copper-mediated Giese-type coupling reaction with regard to both substrates was examined (Scheme 2). In the first part of the scope, various chromone-3-carboxylic acids **1**, encompassing a range of electron-donating and electron-withdrawing functional groups, were evaluated as potential coupling partners (Scheme 2). Chromone-3-carboxylic acids (**1a–1e**) featuring electron-donating groups on the aromatic ring displayed remarkable compatibility with these photoinduced conditions, yielding separable diastereomeric mixtures of desired products **3a–3e** with high efficiency. Similarly, chromone-3-carboxylic acids (**1f–h**) containing electron-withdrawing groups smoothly underwent the reaction under photoinduced LMCT conditions, affording the desired products **3f–3h** as separable diastereomeric mixtures with commendable yields (ranging from 48% to 34%). Furthermore, chromone-3-carboxylic acids bearing two substituents, such as 6,8-dichloride **1i** were obtained as single diastereomers, and those featuring opposite electronic effects (**3j**, obtained as a separable mixture of diastereomers) successfully furnished the corresponding products **3i** and **3j** in moderate yields (40% and 39% yields, respectively). Notably, hydroxy-substituted chromone-3-carboxylic acids **1k** on the position 6 of the aromatic ring gave desired product in 65% yield under the photoinduced LMCT strategy. It is also worth noting that coumarin-3-carboxylic acid **1l** is applicable in the developed methodology to give **3l**.

In the second part of the scope research, we embarked on an extensive exploration of nucleophiles amenable to selective C–H functionalization. Unactivated cyclic alkanes, including cyclooctane, cyclohexane, and cyclopentane (**2m–2o**), emerged as effective coupling partners, showcasing the versatility of this method. Buoyed by these promising results, we turned our

Scheme 3 Chemo- and diastereoselective reduction of **3a** and **3a'**.

attention to various ether substrates for the C–H functionalization reaction. Gratifyingly, not only did 1,4-dioxane exhibit compatibility, but other cyclic and acyclic ethers such as tetrahydrofuran, tetrahydropyran, diethyl ether, ethyl acetate and γ -butyrolactone also proved to be amenable, yielding the corresponding ether-derived chromanones **3p–3t** in moderate to good yields (ranging from 57% to 74%). In almost all cases, no discernible diastereoselectivity was observed, resulting in a 1:1 mixture of products. While the diastereomers of **3p** could be separated through silica gel chromatography, the diastereomers of products **3q–3s** remained inseparable. Subsequently, the products **3a** and **3a'** were subjected to chemo- and diastereoselective reductions of the carbonyl group (Scheme 3). Depending on the conditions employed the reaction afforded alcohol **4a** or dihydrobenzopyran **5a** in 83 and 95% yields, with complete diastereoselectivity.

Furthermore, to emphasize the synthetic utility of this methodology, the scaled up protocol to a 1 mmol scale was successfully developed (see ESI,[†] Table S6). To gain deeper insights into the potential reaction pathway, a series of control experiments were conducted. The addition of 2.0 equivalents of 2,2,6,6-tetramethylpiperidine-1-oxyl (TEMPO), a widely recognized radical scavenger, to the standard reaction mixture resulted in a noticeable reduction in the yield of the desired reaction pathway (Scheme 4a). Electrospray ionization-high-resolution mass spectrometry further revealed that both



Scheme 4 Mechanistic investigations.

chlorine and aliphatic radicals were effectively trapped by TEMPO (see the ESI† for details). These compelling observations strongly indicate the involvement of radical intermediates within the reaction mechanism, substantiating our proposed pathway under the photoinduced ligand-to-metal charge transfer (LMCT) conditions. Based on these results, the mechanism of developed transformation was proposed. The process is initiated by coordination of acetonitrile to copper chloride and ligand transfer from lithium chloride. Irradiation of the complex obtained initiates ligand-to-metal charge transfer resulting in the homolysis of the Cu–Cl bond and chlorine radical formation. It acts as a powerful hydrogen atom transfer reagent, which undergoes a reaction with 1,4-dioxane to give radical **6** and HCl. The newly formed alkyl radical **6** undergoes Giese reaction with chromone-3-carboxylic acid **1a** followed by decarboxylation. Subsequent newly generated more stable radical **7** takes part in the metallization tautomerization process to give corresponding enolate that undergoes photodemetalation that terminates the reaction affording **3** as target product (Scheme 4b).

In summary, our study successfully showcases a photoinduced LMCT approach for achieving site-specific functionalization of carboxylic acid-activated olefins, ultimately leading to the formation of new C–C σ-bonds. This redox-neutral, photo-catalytic alkylation of nonactivated C(sp³)-H bonds under mild conditions represents a synthetically practical and operationally feasible route for the synthesis of 2-substituted chroman-4-ones. The versatility of this reaction was underscored by its successful application to various electron-rich and electron-deficient substrates.

This contribution has been completed while the first author (MM) was the Doctoral Candidate in the Interdisciplinary Doctoral School of TUL, Poland. This work was financially supported by Young Scientists' Fund at the Faculty of Chemistry, Lodz University of Technology W-3D/FMN/8G/2022 (MM).

Conflicts of interest

There are no conflicts to declare.

Notes and references

- 1 J. F. Hartwig and M. A. Larsen, *ACS Cent. Sci.*, 2016, **2**, 281–292.
- 2 J. C. Chu and T. Rovis, *Angew. Chem., Int. Ed.*, 2018, **57**, 62–101.
- 3 (a) P. Gandeepan, T. Müller, D. Zell, G. Cera, S. Warratz and L. Ackermann, *Chem. Rev.*, 2018, **119**, 2192–2452; (b) S. Agasti, T. Pal, T. K. Achar, S. Maiti, D. Pal, S. Mandal, K. Daud, G. K. Lahiri and D. Maiti, *Angew. Chem., Int. Ed.*, 2019, **131**, 11155–11159; (c) T. Naveen, A. Deb and D. Maiti, *Angew. Chem., Int. Ed.*, 2017, **56**, 1111–1115; (d) T. Patra, S. Nandi, S. K. Sahoo and D. Maiti, *Chem. Commun.*, 2016, **52**, 1432–1435; (e) Y. Abderrazak,

- A. Bhattacharyya and O. Reiser, *Angew. Chem., Int. Ed.*, 2021, **60**, 21100–21115.
- 4 R. Jazzaar, J. Hitce, A. Renaudat, J. Sofack-Kreutzer and O. Baudoin, *Chem. – Eur. J.*, 2010, **16**, 2654–2672.
- 5 M. Neetha, S. Saranya, N. Ann Harry and G. Anilkumar, *Chemistry-Select*, 2020, **5**, 736–753.
- 6 R. Trammell, K. Rajabimoghadam and I. Garcia-Bosch, *Chem. Rev.*, 2019, **119**, 2954–3031.
- 7 I. B. Perry, T. F. Brewer, P. J. Sarver, D. M. Schultz, D. A. DiRocco and D. W. MacMillan, *Nature*, 2018, **560**, 70–75.
- 8 L. Capaldo, D. Ravelli and M. Fagnoni, *Chem. Rev.*, 2021, **122**, 1875–1924.
- 9 X.-S. Xue, P. Ji, B. Zhou and J.-P. Cheng, *Chem. Rev.*, 2017, **117**, 8622–8648.
- 10 (a) J. M. Tedder, *Tetrahedron*, 1982, **38**, 313–329; (b) T. Newhouse and P. S. Baran, *Angew. Chem., Int. Ed.*, 2011, **50**, 3362–3374; (c) M. Bietti, *Angew. Chem., Int. Ed.*, 2018, **57**, 16618–16637.
- 11 M. Bietti, *Angew. Chem., Int. Ed.*, 2018, **57**, 16618–16637.
- 12 A. Hu, J.-J. Guo, H. Pan, H. Tang, Z. Gao and Z. Zuo, *J. Am. Chem. Soc.*, 2018, **140**, 1612–1616.
- 13 B. J. Shields and A. G. Doyle, *J. Am. Chem. Soc.*, 2016, **138**, 12719–12722.
- 14 H.-P. Deng, X.-Z. Fan, Z.-H. Chen, Q.-H. Xu and J. Wu, *J. Am. Chem. Soc.*, 2017, **139**, 13579–13584.
- 15 B. D. Ravetz, J. Y. Wang, K. E. Ruhl and T. Rovis, *ACS Catal.*, 2018, **9**, 200–204.
- 16 J. K. Kochi, *J. Am. Chem. Soc.*, 1962, **84**, 2121–2127.
- 17 (a) S. M. Treacy and T. Rovis, *J. Am. Chem. Soc.*, 2021, **143**, 2729–2735; (b) A. S. Mereshchenko, P. K. Olshin, A. M. Karimov, M. Y. Skripkin, K. A. Burkov, Y. S. Tveryanovich and A. N. Tarnovsky, *Chem. Phys. Lett.*, 2014, **615**, 105–110.
- 18 (a) S. T. Saengchantara and T. W. Wallace, *Nat. Prod. Rep.*, 1986, **3**, 465–475; For selected reviews, see: D. M. Flanigan, F. Romanov-Michailidis, N. A. White and T. Rovis, *Chem. Rev.*, 2015, **115**, 9307; (b) K.-S. Masters and S. Bräse, *Chem. Rev.*, 2012, **112**, 3717; B. R. McDonald and K. A. Scheidt, *Acc. Chem. Res.*, 2015, **48**, 1172; (c) D. L. Galinis, R. W. Fuller, T. C. McKee, J. H. II Cardellina, R. J. Gulakowski, J. B. McMahon and M. R. Boyd, *J. Med. Chem.*, 1996, **39**, 4507; (d) Z. H. Mbawambo, M. C. Kapingu, M. J. Moshi, F. Machumi, S. Apers, P. Cos, D. Ferreira, J. P. J. Marais, D. V. Berghe, L. Maes, A. Vlietinck and L. Pieters, *J. Nat. Prod.*, 2006, **69**, 369; (e) K. Picker, E. Ritchie and W. C. Taylor, *Aust. J. Chem.*, 1976, **29**, 2023; (f) D.-L. Zhao, C.-L. Shao, L.-S. Gan, M. Wang and C.-Y. Wang, *J. Nat. Prod.*, 2015, **78**, 286.
- 19 (a) P. N. Moquist, T. Kodama and S. E. Schaus, *Angew. Chem., Int. Ed.*, 2010, **49**, 7096; (b) H. Kikuchi, M. Isobe, M. Sekiya, Y. Abe, T. Hoshikawa, K. Ueda, S. Kurata, Y. Katou and Y. Oshima, *Org. Lett.*, 2011, **13**, 4624–4627; (c) L. F. Tietze, S. Jackenkroll, J. Hierold, L. Ma and B. Waldecker, *Chem. – Eur. J.*, 2014, **20**, 8628–8635; (d) G. Sudhakar, S. Bayya, V. D. Kadam and J. B. Nanubolu, *Org. Biomol. Chem.*, 2014, **12**, 5601–5610.
- 20 D. Genovese, C. Conti, P. Tomao, N. Desideri, M. L. Stein, S. Catone and L. Fiore, *Antiviral Res.*, 1995, **27**, 123–136.
- 21 For reviews on decarboxylative strategies, see: (a) Z.-L. Wang, *Adv. Synth. Catal.*, 2013, **355**, 2745; (b) S. Nakamura, *Org. Biomol. Chem.*, 2014, **12**, 394; (c) J. Bojanowski and A. Albrecht, *Asian J. Org. Chem.*, 2019, **8**, 746.
- 22 (a) M. Moczulski, E. Kowalska, E. Kuśmierk, L. Albrecht and A. Albrecht, *RSC Adv.*, 2021, **11**, 27782–27786; (b) E. Kowalska, A. Artelska and A. Albrecht, *J. Org. Chem.*, 2022, **87**(15), 9645–9653.
- 23 (a) B. Giese, J. A. Gonzalez-Gomez and T. Witzel, *Angew. Chem., Int. Ed. Engl.*, 1984, **23**, 69; (b) J. Rostoll-Berenguer, G. Blay, J. R. Pedro and C. Vila, *Org. Lett.*, 2020, **22**, 8012.